Research Article

iMedPub Journals
http://www.imedpub.com

Nano Research & Applications
ISSN 2471-9838

2017
Vol. 3 No. 2 : 6

DOI: 10.21767/2471-9838.100023

General Encapsulation of Core-Shell Nanoparticles by Metal Nanoshell in Colloids

Xiaohui Song[1], Cuicui Liu[2], Songlin Liu[2] and Weichang Xu[2]

1 Department of Materials Science and Engineering, University of Illinois, Urbana, Illinois, USA
2 Division of Chemistry and Biological Chemistry, Nanyang Technological University, Singapore

Corresponding author: Dr. Xiaohui Song

xiaohui@illinois.edu

General Encapsulation of Core-Shell Nanoparticles by Metal Nanoshell in Colloids.

Tel: +12173331441

Citation: Song X, Liu C, Liu S, et al. General Encapsulation of Core-Shell Nanoparticles by Metal Nanoshell in Colloids. Nano Res Appl. 2017, 3:2.

Abstract

We demonstrate the use of Au@PSPAA core-shell nanoparticles as seeds to grow metal nanoshell in colloidal system which is a facile and general method. The shell thickness and roughness were controlled by several factors, such as the type of surfactant, the ligand concentration, the quantity of the precursor, and the type of reducing agent. Different kinds of metal nanoshell encapsulation hase been achieved in colloidal system which is critical to its further optial perperties study. We believe that the present method could be applied to fabricate/design more complex and anisotropic particles containing multi shells and the relative applications.

Keywords: Nanoparticle; Coating; Core-shell; Colloids

Received: April 27, 2017; **Accepted:** June 02, 2017; **Published:** June 05, 2017

Introduction

The synthesis of nanoparticles and other nanostructures has received considerable attention in these years, since their properties, such as optical, mechanical, and chemical properties, depend strongly on their size, their geometric structures and components, which are quite different from that of bulk materials [1-6]. Because of this dependence, researchers can prepare specific nanomaterials with desired properties, and also can endow the nanomaterials with multiple properties or new properties by combining nanomaterials with different properties together [7-10].

One typical example is metal nanoshells, which are a new class of nanoparticles with highly tunable optical properties, consisting of a dielectric (silica, Polystyrene, Au_2S, Fe_2O_3) core (40 nm to 250 nm radius) surrounded by a thin (10 nm to 30 nm) metallic shell (Au, Ag) [10-14]. Metal nanoshells exhibit a strong plasmon-derived optical resonance, which can shift to much longer wavelengths than that of the corresponding metal nanoparticles, allowing materials to be specifically designed to match the wavelength required for a particular application, for instance to fall within near infrared (NIR) regions where light penetration through tissue is optimal [10,15].

There are several methods for preparation of such metal nanoshell. The most commonly used one was developed by Halas and co-workers, who made gold nanoshells on silica nanoparticles (NPs) with Au nanoseeds attachment [16-18]. Typically, silica NPs were first modified with (3-aminopropyl) trimethoxysilane, followed by immobilizing the small Au nanoseeds (2 nm) onto the surface of silica NPs. The Au nanoseeds could act as the nucleation sites for the Au deposition in the following process of reducing the Au precursor. The other method exploited the direct overgrowth of Au nanoshell on a hybrid nanostructures consisting of AuNPs and polystyrene (PS) NPs without the self-nucleation of Au . In our precursor. The other method exploited the direct overgrowth of Au nanoshell on a hybrid nanostructures consisting of AuNPs and polystyrene (PS) NPs without the self-nucleation of Au [19]. In our previous work, we have synthesized AuNPs encapsulated with amphiphilic block copolymer PS_m-*b*-PAA_n (AuNP@PSPAA) successfully, which has the AuNP as the core, PS as the shell, and PAA as the corona dissolved in the solvent [5,20-23]. However, in these reported method, the core materials were generally limited to silica, PS, Au_2S and Fe_2O_3.

In this study, a general method was developed to make various metal nanoshells growing on the surface of AuNP@PSPAA. And also, the corresponding optical properties of this AuNP@PSPAA@ metal nanoshell have been tested.

Materials and Methods

All chemical reagents were used as purchased without further purification. Hydrogen tetrachloroaurate(III) hydrate ($HAuCl_4$, 99.9%, metal basis Au 49%), sodium palladium tetrachloride (Na_2PdCl_4), hydrogen tetrachloroplatinate(II) (H_2PtCl_4), and ruthenium chloride ($RuCl_3$) were purchased from Alfa Aesar; Indium(III) nitrate hydrate ($In(NO_3)_3 \cdot xH_2O$), silver nitrate ($AgNO_3$), cetyl trimethylammonium bromide (CTAB), sodium citrate (NaCt), polyvinylpyrrolidone (PVP, K-30), tetrakis(hydroxymethyl) phosphonium Chloride (THPC), and poly(allylamine hydrochloride) (PAH) were purchased from Sigma-Aldrich. Amphiphilic diblock copolymer polystyrene-*block*-poly (acrylic acid) (PS_{154}-*b*-PAA_{49}, M_n=16000 for PS block and M_n=3500 for PAA block, M_w/M_n=1.15) was purchased from Polymer Source, Inc. Sodium hydroxide (NaOH) was purchased from Sinopharm Chemical Reagent Co. ltd. 2-Dipalmitoyl-sn-glycero-3-phosphothioethanol (PS-H) was purchased from Avanti Polar Lipids. The negatively charged, citrate-stabilized AuNPs (15 nm and 40 nm) [22] were prepared following literature procedures. Deionized water (resistance>18.2 MΩ/cm) was used in all reactions. All other chemicals were purchased from Sigma Aldrich. Copper specimen grids (200 mesh) with formvar/carbon support film (referred to as TEM grids in the text) were purchased from Beijing XXBR Technology co. ltd.

Characterization

TEM images were collected on a JEM-1400 (JEOL) Transmission Electron Microscope operated at 100 kV.

Preparation of TEM samples

$(NH_4)_6Mo_7O_{24}$ was used as the negative stain in all of the TEM images in this study. TEM grids were treated with oxygen plasma in a Harrick plasma cleaner/sterilizer for 1 min to improve their surfaces hydrophilicity. A drop of sample solution was carefully mixed with stain solution ($(NH_4)_6Mo_7O_{24}$, 1 *wt*%) on the surface of a Parafilm. Then, the hydrophilic face of the TEM grid was placed in contact with the stained sample solution, and a filter paper was used to wick off the excess solution on the TEM grid. After drying in air, it can be used for TEM characterization.

Method

The method used here was similar to our previous report on single-encapsulation of gold nanoparticles with minor modification [24]. Typically, two 1.5 mL tubes of AuNPs solution (d_{Au}=15 nm) were concentrated to ~10 µL by centrifugation at 14000 *rpm* for 15 min. The deep red solution collected at the bottom of the tubes was dispersed in 190 µL H_2O. Then the mixture was added into 900 µL of polymer solution which was prepared by mixing 820 µL DMF with PS_{154}-*b*-PAA_{49} in DMF (80 µL, 8 mg/mL). Finally, hydrophobic ligand PS-H in EtOH (40 µL, 2 mg/mL) was added into the mixture. The mixture was heated at 110°C for 2 h and then slowly cooled down to room temperature. The similar method was used to encapsulate the 50 nm and 70 nm AuNPs.

Results and Discussion

Firstly, the AuNP@PSPAA was synthesized as previously reported [18,21]. Citrate-stabilized AuNPs (50 nm) were first modified with hydrophobic ligand, 1,2-dipalmitoyl-*sn*-glycero-3-phosphothioethanol (PS-H). The amphiphilic block copolymer PSPAA then self-assembled on the surface of AuNP, forming a uniform PSPAA shell **(Scheme 1)**. The AuNP@PSPAA was purified 2 times by centrifugation to remove the empty PSPAA micelles and excess DMF. To get the positively charged AuNP@PSPAA, the purified nanoparticles were then re-dispersed in H_2O (pH 10), followed by addition of positive PAH aqueous solution. After incubating the mixture at RT overnight to facilitate the ligand attachment, the positively charged AuNP@PSPAA was formed. The positively charged AuNP@PSPAA was purified 2 times again by centrifugation to remove the excess PAH, and re-dispersed in H_2O for the further use. Finally, to attach the Au nanoseeds (NS) onto the surface of AuNP@PSPAA, the negatively charged NS were prepared separately and then mixed with the aqueous solution of the positively charged AuNP@PSPAA in a desired ratio, and allowed to age for a controlled time. After that, the AuNP@PSPAA@NS was formed and can be used in the following step after purification by centrifugation. As shown in **Figure 1a, 1b, 1c**, the small dark dots (NSs) attached on the PSPAA shell can be clearly observed and the NSs' size was around 1 nm. The NSs distributed uniformly on the PSPAA shell with high density. The UV-vis absorption spectra of the AuNP@PSPAA and AuNP@PSPAA@NS in water were measured. As shown in **Figure 1d**, there is no obvious change of absorption between these two samples, which means that during the preparation process, there is no aggregation of AuNP@PSPAA occurred. However, because of the loss of AuNP@PSPAA during 4 times of purification process, the intensity of the absorption was decreased sharply from AuNP@PSPAA to AuNP@PSPAA@NS.

When CTAB was used as the surfactant in the synthesis of Au nanoshell on AuNP@PSPAA, it is difficult to get the continuous shell on the AuNP@PSPAA. Typically, AuNP@PSPAA@NS solution was mixed with CTAB solution, followed by addition of $HAuCl_4$ solution and reducing agent ascorbic acid. The color of the solution changed quickly from light red to light purple once the ascorbic acid was injected into the mixture. When the size of AuNP (AuNP@PSPAA) was 15 nm, two types of nanostructures

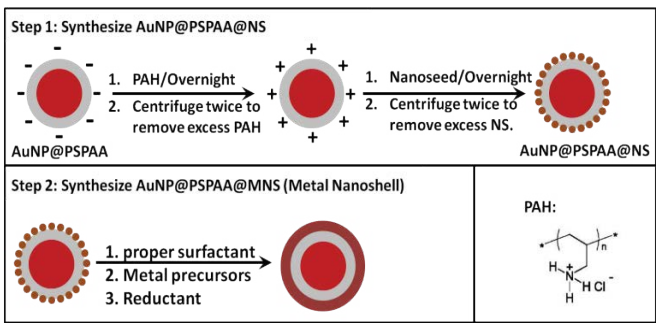

Scheme 1 Schematics showing a general Method for growing Metal Nanoshells (MNS) on AuNP@PSPAA Core.

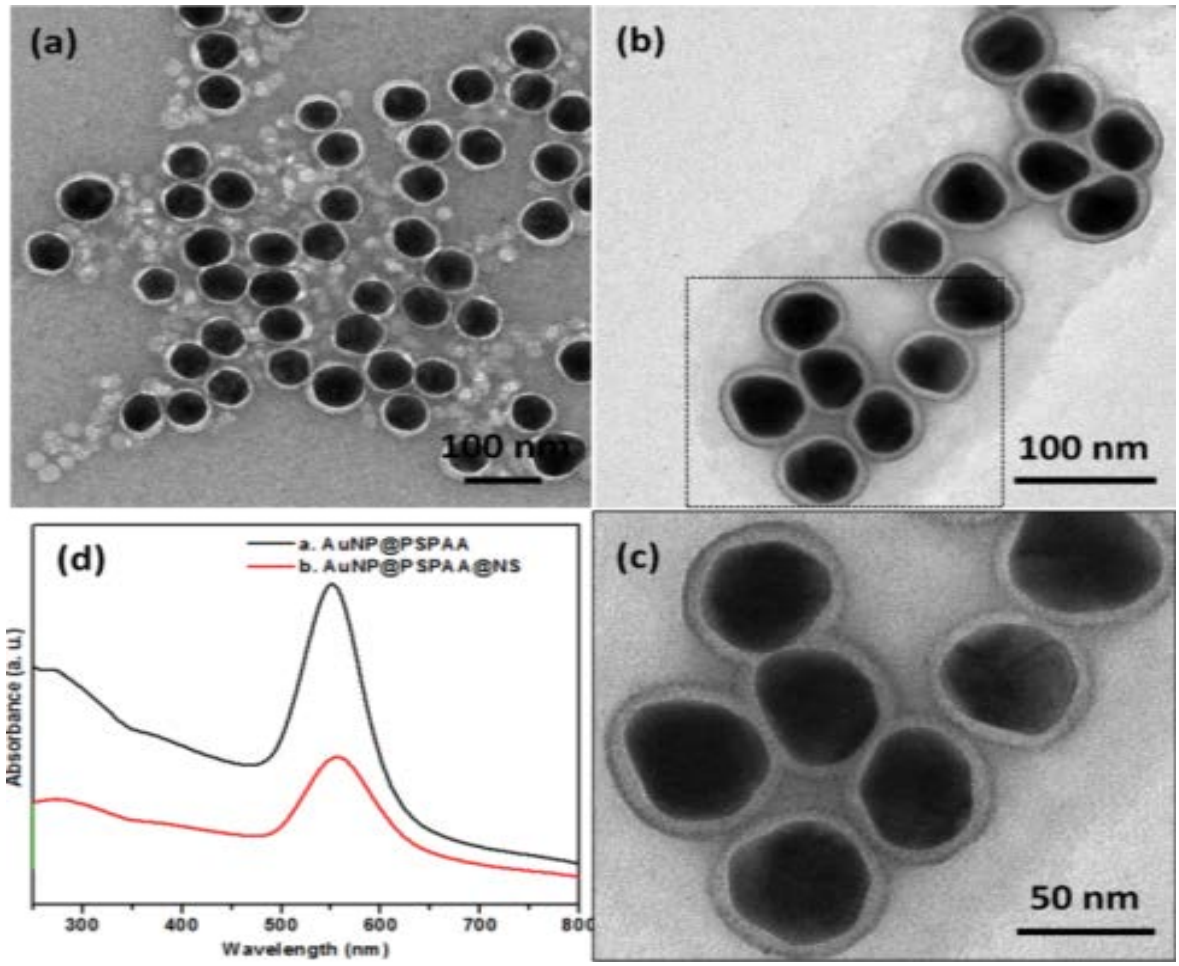

Figure 1 TEM images of (a) AuNP@PSPAA, (b) AuNP@PSPAA@NS, (c) enlarged image of the marked area in (b); (d) UV-vis absorption spectra of (a) AuNPs@PSPAA and (b) AuNPs@PSPAA@NS.

were achieved: 1) one AuNP satellite on one AuNP@PSPAA (**Figure 2a)**, which was synthesized under the gentle experimental condition: The reaction solution was gently shook with hand after addition of all reactants; 2) several AuNP satellites on one AuNP@PSPAA which was synthesized under the harsh experimental condition: The reaction solution was vigorously shook by vortex after addition of all reactants. Maybe because the size of AuNP@PSPAA was too small, its high curvature was not favorable for the formation of continuous shell. We used larger size AuNP (70 nm) instead of the small one, and found that similar structures were formed: plenty of AuNP satellites on the AuNP@PSPAA core. Enlarged TEM image showed that the size of AuNP satellites was around 20 nm, and the density of the satellites was very high. So, under this experimental condition, we could not obtain the AuNP@PSPAA with continuous shell. From the literature, it is known that the CTAB has good affinity to the (110) facet of AuNP [25-27]. Maybe due to this reason, the AuNP satellites could not fuse together to form the continuous shell.

When negatively charged sodium citrate was used as surfactant in this system, continuous Au nanoshell could grow on the surface of AuNP@PSPAA, as shown in **Figure 2c**. The AuNP core and Au nanoshell appear black in TEM image while the colour of PSPAA domain in between them was grey, because the polymer part can create a "spacer" in the path of the electron beam. According to **Figure 2c**, it is obvious that the Au nanoshell is continuous smooth shell. In addition, a lot of smaller AuNPs were synthesized from the self-nucleation process, which was hard to prevent in this system. The surface roughness of the Au nanoshell on the AuNP@PSPAA can be controlled by adding ligand into the reaction. As shown in **Figure 2d**, when a small amount of 4-MBA (4-mercaptobenzoic acid) was added into the system, the Au nanoshell with rough surface was easily achieved. The more ligand added, the rougher surface the Au nanoshell presents **(Figure 2e and 2f)**. The phenomenon can be explained by the theory reported in our previous paper: the strong binding property of 4 MBA in this system forces selective deposition of Au at the ligand-deficient interface between Au NSs and PSPAA domain to form dense Au nanoworms, resulting in the rough surface [28-30].

Besides the growth of Au nanoshells on AuNP@PSPAA, we can extend this method to grow other metal/metal oxide nanoshells (e. g. Ag, Pt, Pd. Rh, $In(OH)_3$) on AuNP@PSPAA. Taking Ag nanoshell growth as an example, the AuNP@PSPAA@Ag nanoshell synthesized in our system **(Figure 3a and 3b)** is

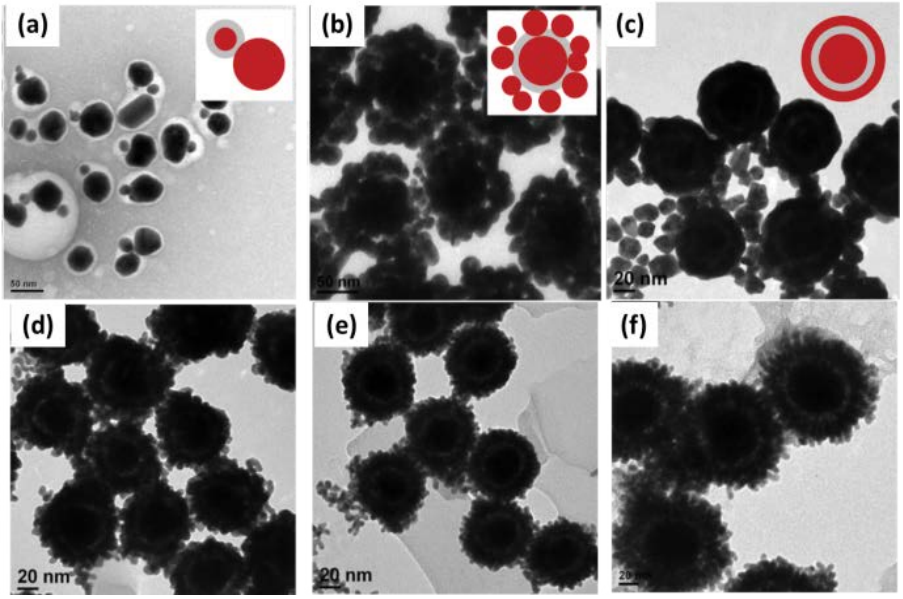

Figure 2 TEM images of Au@PSPAA coated by Au nanoshell at the presence of different ligands/surfactant: **(a)** CTAB, **(b)** 4-MBA, **(c)** Sodium citrate; **(d)** 4-MBA 1 mM, 10 µL + sodium citrate, **(e)** 4-MBA 1 mM, 30 µL + sodium citrate, and **(f)** 4-MBA 1 mM, 40 µL + sodium citrate.

attractive for use as a SERS substrate. In order to evaluate the performance of this structure for SERS application, 4-MBA was used as probe molecules because it can be adsorbed on the surface of AgNP easily and has enormous intensity enhancement [31]. A certain amount of 4-MBA was introduced into the solution before the addition of $AgNO_3$ and ascorbic acid. The addition of 4-MBA did not have significant influence on the final morphologies. When the concentration of 4-MBA in the solution reached 1 µM **(Figure 3c)**, the highest SERS enhancement was achieved. Above this critical concentration, the SERS signal kept unchanged. It is known that SERS exceptionally strong in the gap between plasmon-coupled metal nanoparticles (NPs), which is called SERS "hotspots" [32-34]. In our system, the "Ag nanoshell" was constructed from a lot of AuNPs. Therefore, plenty of SERS "hotspots" exsited in between the AgNPs, which can employ as the container for the 4-MBA. Maybe due to the limited capacity of such "container", the higher concentration of the 4-MBA did not result in the stronger SERS signals. **Figure 4a-4f** show that the Pt, Pd, Rh, and in $(OH)_3$ nanoshells respectively synthesized by similar method. From the literature, it is known that Pt required higher temperature to be reduced from the precursor H_2PtCl_4, since the primary nucleation of Pt nanoparticles needed to conquer significant energy barrier [35,36]. However, because of the existence of NSs (Au nanoseeds) in our system **(Figure 4a and 4b)**, the growth of Pt on NSs was favoured even at room temperature [37]. **Figure 4c and 4d** showed the typical TEM images of the AuNP@PSPAA@Pd nanoshell with thickness 30 nm. **Figure 4e** showed the typical TEM image of AuNP@PSPAA@ Rh nanoshell, where the Rh nanoshell consisted of hair-like nanostructures. The yield of this product was relatively low, since plenty of RhNPs were formed from the self-nucleation process. Finally, TEM images of AuNP@PSPAA@ $In(OH)_3$ nanoshell [38]

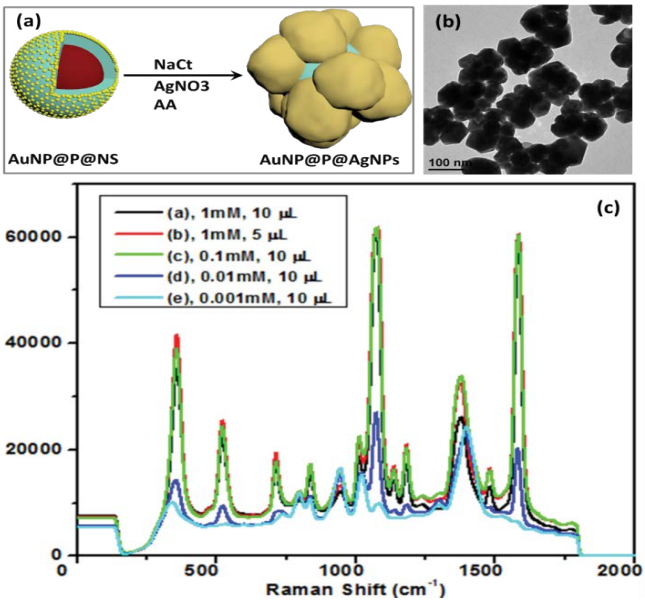

Figure 3 (a) Scheme of AuNP@PSPAA with Ag metal nanoshells:, and (b) TEM images (c) Raman spectra of Au NP@ PSPAA@Ag nanoshell particles with the different 4-MBA concentration.

were shown in **Figure 4f**. The enlarged image showed that there were plentiful white dots in the in $(OH)_3$ nanoshell, indicating that the nanoshell was mesoporous.

Conclusion

In summary, we systematically studied the metal nanoshell growth in colloidal system giving different types of metal

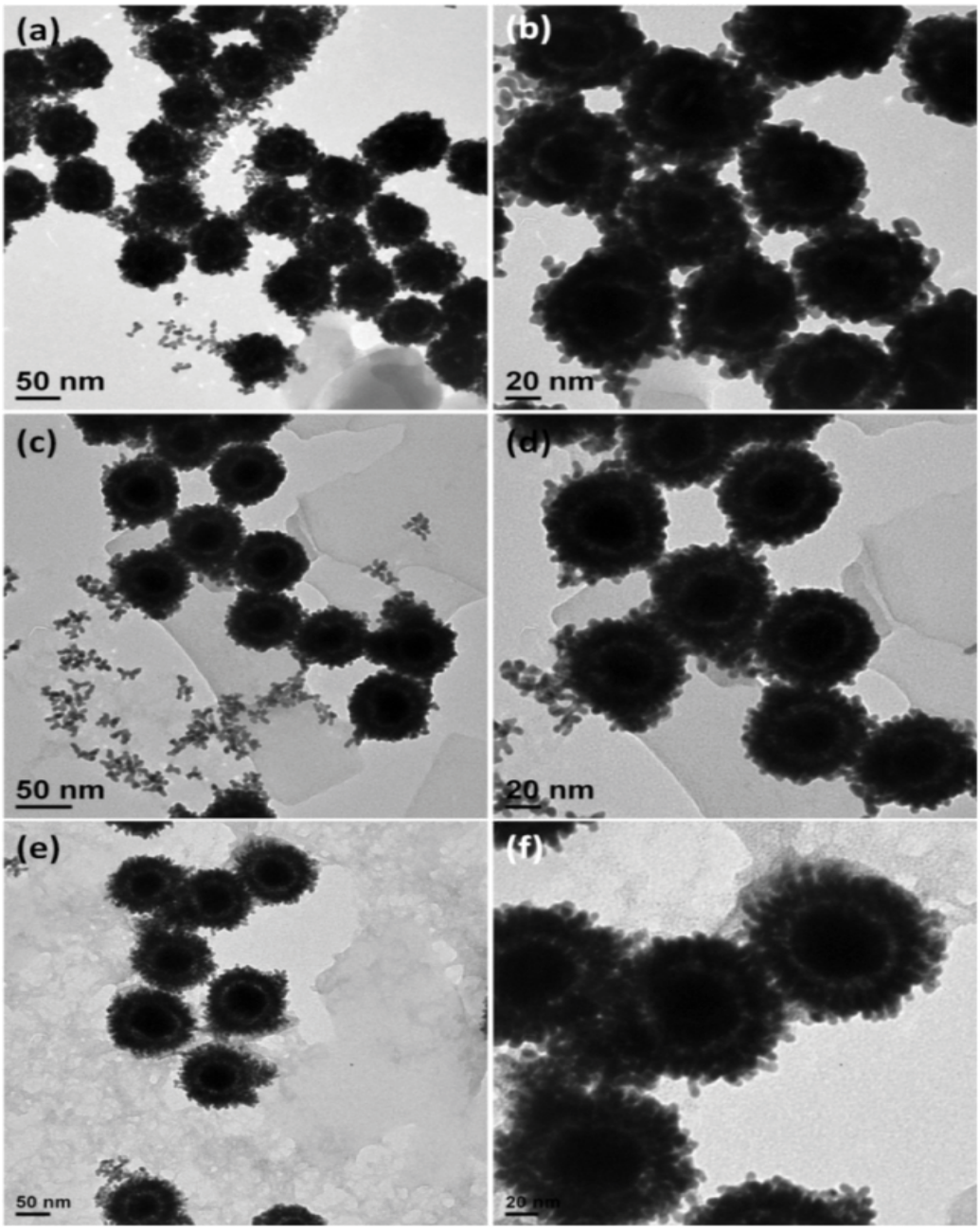

Figure 4 TEM images of AuNP@PSPAA (50 nm AuNP) with different metal nanoshells: (a, b) Pt; (c, d) Pd; (e) Rh, (f) $In(OH)_{3a}$.

nanoshells, such as smooth shell, flower shell and rough cluster shell. The ligands molecule type, ligands concentration, as well as metal-ligand bonding effects have been studied. A general and facile method has been developed which could be applied to different kinds of cores and metal shells. This novel method opens door to complex nanoparticles design and its optical properties study.

Funding

There is no interest conflict.

References

1 Liu NG, Prall BS, Klimov VI (2006) Hybrid Gold/Silica/Nanocrystal-quantum-dot superstructures: Synthesis and analysis of semiconductor-metal interactions. J Am Chem Soc 128: 15362-15363.

2 Lee JH, Kim GH, Nam JM (2012) Directional synthesis and assembly of bimetallic nanosnowmen with DNA. J Am Chem Soc 134: 5456-5459.

3 Zeng J, Zhu C, Tao J, Jin MS, Zhang H, et al. (2012) Controlling the nucleation and growth of silver on palladium nanocubes by manipulating the reaction kinetics. Angew Chem Int 51: 2354-2358.

4 Zhang H, Li YJ, Ivanov IA, Qu YQ, Huang Y, et al. (2010) Plasmonic modulation of the upconversion fluorescence in NaYF4 :Yb/Tm hexaplate nanocrystals using gold nanoparticles or nanoshells. Angew Chem Int Edit 49: 2865-2868.

5 Wang H, Chen L, Feng Y, Chen H (2013) Exploiting core-shell synergy for nanosynthesis and mechanistic investigation. Acc Chem Res 46: 1636-1646

6 Yang P, Zheng J, Xu Y, Zhang Q, Jiang L (2016) Colloidal synthesis and applications of plasmonic metal nanoparticles. Adv Mater 28: 10508-10517.

7 Jin YD, Gao XH (2009) Plasmonic fluorescent quantum dots. Nat Nanotechnol 4: 571.

8 Hu SH, Gao X (2010) Stable encapsulation of quantum dot barcodes with silica shells. Adv Funct Mater 20: 3721-3726.

9 Deng YH, Cai Y, Sun ZK, Liu J, Liu C, et al. (2010) Multifunctional mesoporous composite microspheres with well-designed nanostructure: A highly integrated catalyst system. J Am Chem Soc 132: 8466-8473.

10 Halas NJ, Lal S, Chang WS, Link S, Nordlander P (2011) Plasmons in strongly coupled metallic nanostructures. Chem Rev 111: 3913-3961.

11 Zhang P, Guo YY (2009) Surface-enhanced raman scattering inside metal nanoshells. J Am Chem Soc 131: 3808-3809.

12 Bardhan R, Grady NK, Ali T, Halas NJ (2010) Metallic nanoshells with semiconductor cores: Optical characteristics modified by core medium properties. ACS Nano 4: 6169-6179.

13 Wang H, Brandl DW, Le F, Nordlander P, Halas NJ (2006) Nanorice: A hybrid plasmonic nanostructure. Nano Lett 6: 827-832.

14 Wang X, Feng J, Bai Y, Zhang Q, Yin Y (2016) Synthesis, properties, and applications of hollow micro-/nanostructures. Chem Rev 116: 10983-11060.

15 Yang PP, Xu Y, Chen L, Wang XC, Mao BH, et al. (2015) Encapsulated silver nanoparticles can be directly converted to silver nanoshell in the gas phase. Nano Lett 15: 8397-8401

16 Jackson JB, Halas NJ (2001) Silver Nanoshells: Variations in morphologies and optical properties. J Phys Chem B 105: 2743-2746.

17 Pham T, Jackson JB, Halas NJ, Lee TR (2002) Preparation and characterization of gold nanoshells coated with self-assembled monolayers. Langmuir 18: 4915-4920.

18 Hirsch LR, Gobin AM, Lowery AR, Tam F, Drezek RA, et al. (2006) Metal nanoshells. Ann Biomed Eng 34: 15-22.

19 Jeong E, Kim K, Choi I, Jeong S, Park Y, et al. (2012) Three-dimensional reduced-symmetry of colloidal plasmonic nanoparticles. Nano Lett 12(9): 2436-2440.

20 Chen HY, Abraham S, Mendenhall J, Delamarre SC, Smith K, et al. (2008) Encapsulation of single small gold nanoparticles by diblock copolymers. ChemPhysChem 9: 388-392.

21 Chen G, Wang Y, Tan LH, Yang MX, Tan LS, et al. (2009) High-purity separation of gold nanoparticle dimers and trimers. J Am Chem Soc 131:4218-4219.

22 Tan LH, Xing SX, Chen T, Chen G, Huang X, et al. (2009) Fabrication of polymer nanocavities with tailored openings. ACS Nano 3: 3469-3474.

23 Yang MX, Chen T, Lau WS, Wang Y, Tang QH, et al. (2009) evelopment of polymer-encapsulated metal nanoparticles as surface-enhanced raman scattering probes. Small 5: 198-202.

24 Frens G (1973) Controlled nucleation for the regulation of the particle size in monodisperse gold suspensions. Nat Phys Sci 241: 20-22.

25 Wang H, Song XH, Chen HY (2014) Homo- and Co-polymerization of nanoparticles. ACS Nano 8: 8063

26 Ha TH, Kim YJ, Park SH (2010) Complete separation of triangular gold nanoplates through selective precipitation under CTAB micelles in aqueous solution. Chem Commun 46: 3164-3166.

27 Nikoobakht B, El-Sayed MA (2003) Preparation and growth mechanism of gold nanorods (NRs) using seed-mediated growth method. Chem Mater 15: 1957-1962.

28 He JT, Wang YW, Feng YH, Qi XY, Zeng Z, et al. (2013) Forest of gold nanowires: A new type of nanocrystal growth. ACS Nano 7: 2733-2740.

29 Lim DK, Kim IJ, Nam JM (2008) DNA-embedded Au/Ag core-shell nanoparticles. Chem Commun 42: 5312-5314.

30 Chen HJ, Kern E, Ziegler C, Eychmuller A (2009) Ultrasonically assisted synthesis of 3D hierarchical silver microstructures. J Phys Chem C 113: 19258-19262.

31 Liu XH, Zhou LB, Yi R, Zhang N, Shi RR, et al. (2008) Single-crystalline indium hydroxide and indium oxide microcubes: Synthesis and characterization. J Phys Chem C 47: 18426-18430

32 Chen G, Wang Y, Yang MX, Xu J, Goh SJ, et al. (2010) Measuring ensemble-averaged surface-enhanced raman scattering in the hotspots of colloidal nanoparticle dimers and trimers. J Am Chem Soc 132: 3644-3645.

33 Xu HX, Bjerneld EJ, Kall M, Borjesson L (1999) Spectroscopy of single hemoglobin molecules by surface enhanced Raman scattering. Phys Rev Lett 83: 4357.

34 Hao E, Schatz GC (2004) Electromagnetic fields around silver nanoparticles and dimers. J Chem Phys 120: 357-366.

35 Zhang HT, Ding J, Chow GM (2008) Morphological control of synthesis and anomalous magnetic properties of 3D branched Pt nanoparticles. Langmuir 24: 375-378.

36 Lacroix LM, Gatel C, Arenal R, Garcia C, Lachaize S, et al. (2012) Tuning complex shapes in platinum nanoparticles: From cubic dendrites to fivefold stars. Angew Chem Int Edit 51: 4690-4694.

37 Johnson CJ, Dujardin E, Davis SA, Murphy CJ, Mann S (2002) Growth and form of gold nanorods prepared by seed-mediated, surfactant-directed synthesis. J Mater Chem 12: 1765-1770.

38 Feng YH, Wang Y, Wang H, Chen T, Tay YY, et al. (2012) Engineering "hot" nanoparticles for surface-enhanced Raman scattering by embedding reporter molecules in metal layers. Small 8: 246-251.